Check for updates

Geophysical Research Letters

RESEARCH LETTER
10.1029/2024GL110130

Scattering Evidence for an Ancient Subducted Slab Using the Unique Raypath P*PKP

Hao Zhang[1], **John E. Vidale**[1], **and Wei Wang**[2,3]

[1]Department of Earth Sciences, University of Southern California, Los Angeles, CA, USA, [2]Key Laboratory of Earth and Planetary Physics, Institute of Geology and Geophysics, Chinese Academy of Sciences, Beijing, China, [3]College of Earth and Planetary Sciences, University of Chinese Academy of Sciences, Beijing, China

Key Points:

- A unique raypath P*PKP is utilized to detect heterogeneities in the mantle
- Strong scattering coincides with a hypothesized ancient subducted slab beneath the Indian Ocean
- This Southeast Indian Slab may have stagnated more than 100 Ma, which is unusually long

Supporting Information:

Supporting Information may be found in the online version of this article.

Correspondence to:

H. Zhang,
hzhang63@usc.edu

Citation:

Zhang, H., Vidale, J. E., & Wang, W. (2024). Scattering evidence for an ancient subducted slab using the unique raypath P*PKP. *Geophysical Research Letters*, *51*, e2024GL110130. https://doi.org/10.1029/2024GL110130

Received 8 MAY 2024
Accepted 11 SEP 2024

Author Contributions:

Conceptualization: Hao Zhang, John E. Vidale, Wei Wang
Data curation: John E. Vidale, Wei Wang
Formal analysis: Hao Zhang, John E. Vidale
Funding acquisition: John E. Vidale
Investigation: Hao Zhang, John E. Vidale
Methodology: Hao Zhang, John E. Vidale, Wei Wang
Project administration: John E. Vidale
Resources: John E. Vidale
Software: Hao Zhang, John E. Vidale, Wei Wang
Supervision: John E. Vidale
Validation: Hao Zhang, John E. Vidale, Wei Wang
Writing – original draft: Hao Zhang
Writing – review & editing: Hao Zhang, John E. Vidale, Wei Wang

© 2024. The Author(s).
This is an open access article under the terms of the Creative Commons Attribution License, which permits use, distribution and reproduction in any medium, provided the original work is properly cited.

Abstract We observe high-frequency scatterers consistent with the interpretation of a tabular high-velocity structure under the Indian Ocean as an ancient subducted slab. We use a previously rarely used raypath, P waves scattered in the slab into PKP waves (P*PKP), from 12 earthquakes and explosions in five locations recorded on the antique LASA (Large Aperture Seismic Array) located in Montana, United States. The scatterers concentrate in the mantle transition zone and ~1,500 km depths, in the locations where the fast anomalies in the tomography broaden and strengthen. Our inference that the slab lingers in the upper- and mid-mantle despite subducting and detaching more than 130 million years ago suggests that models of slabs sinking into the mantle may have to accommodate such long-term stagnation.

Plain Language Summary Through study of a novel raypath of seismic waves identified on a large, high-quality seismographic array, we find evidence of an ancient subducted slab residing beneath the Indian Ocean. Our investigation reveals the presence of high-frequency scatterers nestled approximately 500 and 1,500 km deep. Notably, these scatterers locate within fast anomalies observed in tomographic imaging. Despite having undergone subduction and detachment over 130 million years ago, this slab remains suspended mid-mantle. Such longevity challenges prevailing models of subduction dynamics by indicating protracted stagnation of subducted lithospheric material within the Earth's mantle.

1. Introduction

Lithospheric plates, subducting into the mantle, may either stagnate in the mantle transition zone or penetrate through to the lower mantle, where they may also stall (Goes et al., 2017). Understanding these varying behaviors of subducted slabs helps evaluate past tectonic history through valuable insights into mantle properties such as viscosity and thermal phase transitions. The observation of subducted plates relies on seismic constraints, which have broadened from simply Wadati-Benioff seismicity (Isacks & Molnar, 1971) to modern models derived from global/regional tomography (Lay, 1994; Wei et al., 2020) and seismic scattering locations (Kaneshima, 2016). Favorable coverage by seismic ray paths is crucial for these seismological analyses. In particular, ancient subduction slabs within the interiors of modern plates remain under-constrained, leaving the comprehensive history and mechanics of mantle circulation open to debate.

One such ancient subduction slab, the Southeast Indian Slab (SEIS), was recently identified in a global tomography model beneath the Indian Ocean (Simmons et al., 2012, 2015). The SEIS reveals a regionally slab-like structure between the Kerguelen Plateau and Java, Indonesia. This slab dips northward, extending from the upper mantle down to the core-mantle boundary (CMB). The SEIS is positioned above the African large low-shear-velocity province (LLSVP) and aligns with the location of the Indian geoid low. Based on a regional tectonic reconstruction, the SEIS is inferred to have subducted prior to the breakup of East Gondwana (130–140 Ma) (Gibbons et al., 2013). The dip polarity of present-day SEIS suggests either a stagnation period of over 100 Ma, longer than any other known slab, or else a flip in slab polarity flip driven by upwelling mantle flow from the African large low-shear-velocity province (LLSVP) (H. Wang et al., 2018). While both mechanisms are plausible in geodynamic simulations, additional direct observational evidence is necessary to corroborate the possibility of such a persistently stagnant slab. Unfortunately, the SEIS is located beneath a vast gap in seismic observation in the Southern Hemisphere (Kaneshima, 2016). Although hints of the feature are observed in multiple global tomography models developed through decades (Becker & Boschi, 2002; Grand, 2002; Zhao et al., 2013), their resolution has not yet been sufficient to confidently resolve a detailed slab structure (Simmons et al., 2012).

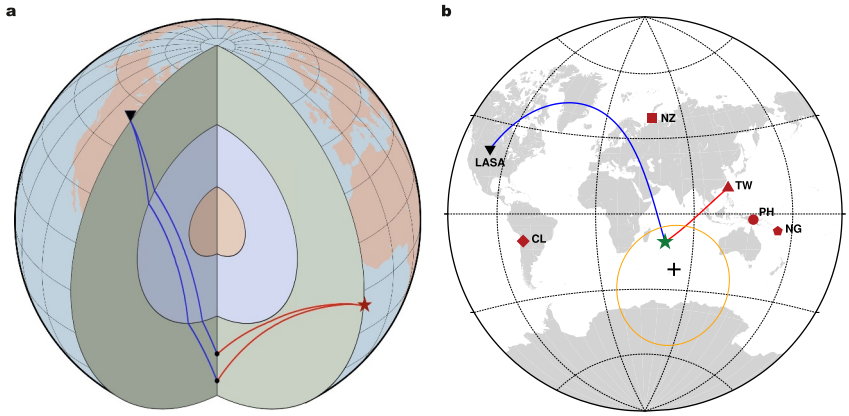

Figure 1. (a) An illustration of the P*PKP path of observed scattered waves. The scattered waves propagate as P waves (red lines) to their scattering points in the mantle (black dots), where they scatter off-plane, converting to the PKP raypath (blue lines) until reaching the array (black triangle). Two scatterers at distinct depths are presented as examples. Note that the scattering point is not in general aligned with Earth's rotation pole as depicted here. (b) Map of the events (red markers) and the LASA array (black triangle) used in this paper. The black cross marks the antipode of LASA, while the yellow circle is the geographical limit of possible scatterers at 500 km depth of PKP from LASA. The green star with raypaths shows an example of scatterers.

Long-term mechanical mixing of the subducted oceanic lithosphere and mantle, combined with phase transitions accompanying slab descent, can induce short-wavelength heterogeneities and small-scale scatterers (Mao et al., 2022). Mantle heterogeneity beneath subduction zones has been observed pervasively in the Marianas (Kaneshima, 2003; Korenaga, 2015), Izu-Bonin (Castle & Creager, 1999; Niu et al., 2003), Japan Sea (Niu, 2014; J. Li & Yuen, 2014), Tonga (Kaneshima, 2013; Yang & He, 2015), and other regions around the Pacific. In this study, we utilize scattered P*PKP waves (where * indicates the scatterer) to chart the distribution of scattering points beneath the Indian Ocean. P*PKP has been rarely studied in previous studies (Earle, 2002), thus providing a novel opportunity to locate scatterers within the mantle. Our results reveal scattering points that align with the location of the SEIS, both in the transition zone and the lower mantle, offering direct observational evidence for the presence of a stagnating ancient subduction slab in two distinct depth ranges.

2. Results

The location of the scattering region can be achieved through the analysis of the slowness and arrival times of scattered waves. In this study, we observe P*PKP waves to locate scattering points beneath the Indian Ocean. The P*PKP waves travel as P in the mantle from the source to the heterogeneity, where they scatter off-plane and penetrate through the outer core as PKP to the array (Figure 1). Given the weakness of heterogeneity in the mantle (Tackley, 2002), array processing methods are necessary to detect the faint scattered energy (Rost et al., 2015), and the observation of P*PKP relies on adequate station density and aperture of the array, as well as the appropriate source-receiver geometry. The seismic array that we employ, the Large Aperture Seismic Array (LASA), was operated from 1968 to 1978 and consisted of up to 525 short-period stations installed in 60 m boreholes in firm ground, spanning a 200-km aperture (Frosch & Green, 1966). Additional information regarding LASA can be found in Supplementary Figure 1 in Supporting Information S1 and our previous publications (Vidale, 2019; Wang & Vidale, 2022a, 2022b).

We adopt an approach similar to that employed by W. Wang and Vidale (2022a) applied to eight earthquakes near Taiwan (TW), Chile (CL), the Philippines (PL), and New Guinea (NG), along with 4 Novaya Zemlya, Russia (NZ) blasts. Only source regions with multiple events are considered to ensure the robustness of the results (except for CL). We apply a 1–3 Hz bandpass filter to the seismograms to isolate the coherent scattered energy across the expansive aperture of LASA. This short-period scattering wavefield is sensitive to structure on the order of a few to tens of kilometers, which is comparable to the size and thickness of crustal fragments in the mantle (Niu, 2014). Then we perform beamforming on the seismograms using all available LASA stations, following the method described by W. Wang and Vidale (2022b). Static shifts, on the order of tenths of seconds and determined by aligning the PKIKP waves of an earthquake near the antipode (Vidale, 2019), are applied to

19448007, 2024, 18, Downloaded from https://agupubs.onlinelibrary.wiley.com/doi/10.1029/2024GL110130 by University Of Southern California, Wiley Online Library on [12/11/2025]. See the Terms and Conditions (https://onlinelibrary.wiley.com/terms-and-conditions) on Wiley Online Library for rules of use; OA articles are governed by the applicable Creative Commons License

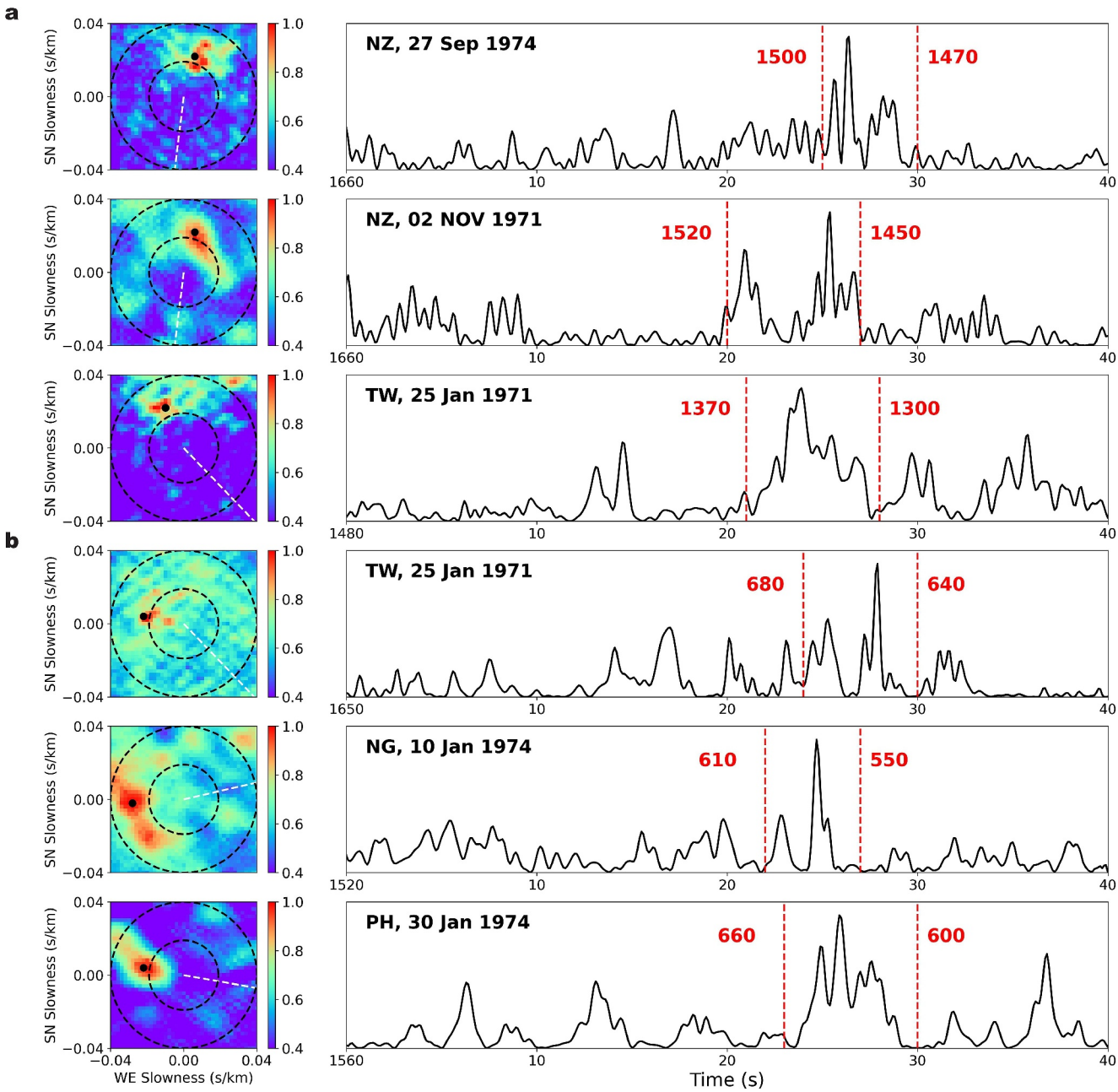

Figure 2. Beams of P*PKP energy emanating from scatterers in the (a) lower mantle and (b) mantle transition zone for representative events, accompanied by the stack envelope at the resolved slowness of P*PKP (black dots). Back azimuth of events are marked using white dashed lines. The delay after event origin time is listed on the left of the stacks. Dashed circles in the slowness beams represent the slowness corresponding to the inner core boundary (ICB) and core-mantle boundary (CMB). Red dashed lines denote the time windows utilized for the slowness beams, with corresponding scatterer depths provided adjacent to them (in kilometers).

account for the arrival perturbation induced by crust and mantle structure beneath LASA. Figure 2 presents beams and corresponding envelopes of stacked waveforms for six events. These beams are plotted in two groups, each exhibiting energy from a similar slowness and azimuth (0.22 s/km from north and 0.21 s/km from west), suggesting a common origin from two strongly scattering regions. All events show scatterers from similar regions; the rest are shown in Supplementary Figures 2–4 in Supporting Information S1.

To evaluate the extent of the strongly scattering region, we utilize a similar back-projection approach as W. Wang and Vidale (2022a) to identify energy peaks in both slowness and time domain based on the single scattering assumption (Cao & Romanowicz, 2007; Frost et al., 2013; Wen, 2000). This method retraces the slowness vector

19448007, 2024, 18, Downloaded from https://agupubs.onlinelibrary.wiley.com/doi/10.1029/2024GL110130 by University Of Southern California, Wiley Online Library on [12/11/2025]. See the Terms and Conditions (https://onlinelibrary.wiley.com/terms-and-conditions) on Wiley Online Library for rules of use; OA articles are governed by the applicable Creative Commons License

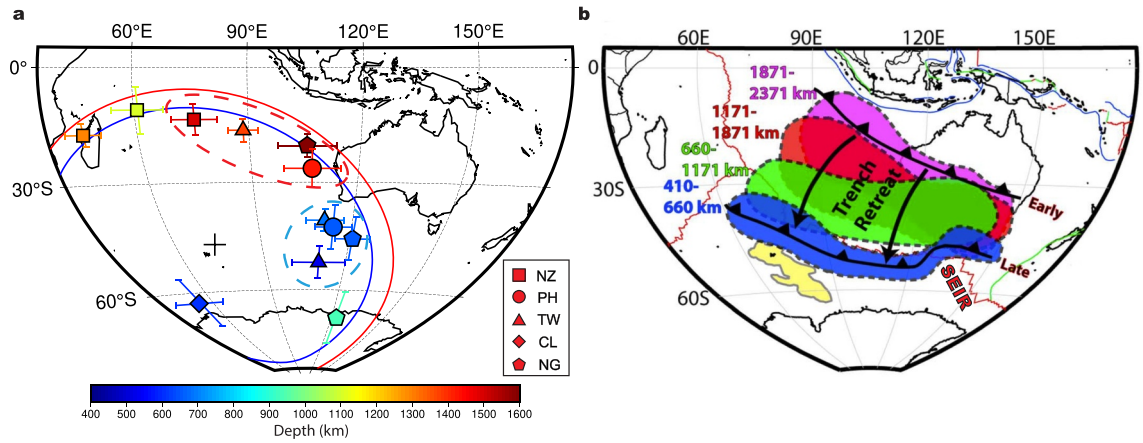

Figure 3. (a) The distribution of scattering points resolved through back-projection analysis with uncertainty, color-coded by depth. The two groups of scatterers in the mantle transition zone and at ~1,500 km depth are encircled by blue and red dashed lines, respectively. Scatterer markers, indicating the events from which they are resolved, correspond to event markers in Figure 1b. The black cross denotes the antipode of LASA. The red and blue rings mark the limit of locations in which scattered arrivals could be observed at 1,500 and 600 km depths, respectively. (b) The location of an ancient subduction slab beneath the present-day Indian Ocean determined by contouring fast shear wave perturbations of >0.25%, as modeled by Simmons et al. (2012). Location of Southeast Indian Ridge (SEIR) is marked using red lines. The Kerguelen Plateau is shown in yellow for reference. Figure after Simmons et al. (2015).

and identifies scatterer locations by matching the IASP91 (Kennet, 1991) prediction of arrival times with observations of prominent bursts, allowing the determination of longitude, latitude, and depth. Comparable to W. Wang and Vidale (2022a), we select the searching regime of slowness large enough to ensure the possible scatterers cover the entire mantle. The uncertainty of the scatterer location is estimated from the 90% peak beam energy contour in the slowness domain (see Supplementary Text 1 in Supporting Information S1 for details), which accounts for both the volume distribution of the scatterer and the array response function (Rost & Thomas, 2002). We examine the seismicity near the LASA array and the scattering region based on the PDE (Preliminary Determination of Epicenters) catalog to eliminate the possibility that these signals are from other earthquakes along the raypath. Our back-projection analysis reveals that the observed P*PKP waves predominantly emanate from two robustly located scattering regions within the mantle beneath the southern Indian Ocean (Figure 3a). The northern region resides at a depth of approximately 1,500 km, while the southern is around 500–600 km deep, in the transition zone. Notably, these regions align closely with the location of the SEIS (Figure 3b), offering direct observational support for the presence of the ancient subducted slab beneath the Indian Ocean. In addition to scattering points associated with the SEIS, we also identified four outlier scatterers. Two of these outliers, situated beneath Madagascar and near the Kerguelen Plateau respectively, were independently identified using longer-period scattered body waves in Rochira et al. (2022), thereby further validating our results.

3. Discussion

Our results provide independent evidence for the existence of the SEIS by the detection of coherent energy from scattered P*PKP waves, a phase rarely documented in the previous literature. Supplementary Figure 5 in Supporting Information S1 shows the traveltime and distance range for P*PKP and other phases that arrive close in space and time. Unlike some previously well-studied scattering probes (e.g., inner core scattering and scattered $P'P'$ waves), the path of P*PKP has a wider distance range available for observation, which samples a fairly large volume of Earth for a given array location. In addition, the wide range of possible distances in the P branch from source to scatterer allows a large set of candidate events to be used. Moreover, P*PKP waves do not necessarily precede or follow other phases, as their path diverges from typical seismic phases, reducing the likelihood of masking effects. Although P*PKP traverses a great distance through the lower mantle and outer core, the attenuation in the lower mantle is weaker compared to the upper mantle (Dziewonski & Anderson, 1981; Romanowicz & Mitchell, 2015), and negligible in the outer core, thereby preserving the scattered energy. Due to the relatively weak heterogeneity in the middle-lower mantle compared to the lithosphere, the observation of P*PKP still relies on array processing methods, for example, the beamforming approach used in this study. Despite this limitation, P*PKP can fill sampling gaps between other phases, which are limited differently by earthquake-station geometry, thereby providing additional information about locations of notable mantle

19448007, 2024, 18, Downloaded from https://agupubs.onlinelibrary.wiley.com/doi/10.1029/2024GL110130 by University Of Southern California, Wiley Online Library on [12/11/2025]. See the Terms and Conditions (https://onlinelibrary.wiley.com/terms-and-conditions) on Wiley Online Library for rules of use; OA articles are governed by the applicable Creative Commons License

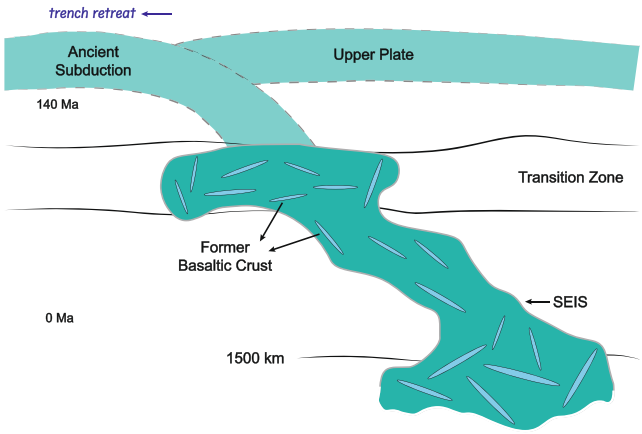

Figure 4. Schematic model showing the ancient subducted slab (SEIS) with accumulations of slab in the area of scattering points. The stagnant slab piles appear as a megalith embedded with pieces of crust. The ancient subduction (transparent part above the transition zone) happened before the breakup of East Gondwana (~140 Ma).

heterogeneity. In this study, we do ray tracing with a one-dimensional layered velocity model to confirm the existence of P*PKP. Given the substantial uncertainty in selecting the optimal slowness for locating the scattering points (see Figure 3), the potential improvement from relocation using high-resolution 3D models, such as LLNL-G3D-JPS (Simmons et al., 2015), may be limited. We plan to implement this in future work.

The observed scattering points in the mantle transition zone and at about 1,500 km depth align with the location of SEIS, though it is hard to determine if these scatterers are located in the middle of the slab or on the slab surface due to the low resolution of the velocity model and large uncertainty of the location. As noted above, small-scale scatterers in close proximity to subduction slabs have been widely documented. These scatterers are attributed to the presence of former basaltic oceanic crust, which generates short-wavelength physicochemical heterogeneities in both middle and lower mantle when mixed with the mantle material during subduction (Ishii et al., 2022; Ringwood & Irifune, 1988; Xu et al., 2008). The absence of detectable scattering from 700 to 1,300 km is intriguing, potentially related to the long-term stagnation history at the mantle transition zone and/or the rapid sinking below the mantle transition zone (Shi et al., 2019). The energy associated with scattered phases is typically weak and its observability is a combined effect of factors such as the amplitude of the heterogeneity (e.g., velocity and density anomaly), the angle of incidence and exit at the scatterer as well as the shape of scatterers. We conceptualize the scatterer as a slab pile resembling a megalith composed of oceanic crust relics (Niu, 2014; Ringwood & Irifune, 1988), where each remnant piece serves as a seismic wave reflector. The stagnation of the slab can lead to the accumulation of crustal pieces and disrupt their down-dip *en echelon* arrangement (Agrusta et al., 2018; Gerya et al., 2021), thereby enhancing the likelihood of observing scattered waves in diverse directions (Figure 4). In accordance with this model, our results suggest that the stagnation of SEIS is happening in both the mantle transition zone and the lower mantle at a depth of 1,500 km. In the downgoing section of the slab between the MTZ and 1,500 km depth, the fragments are aligned parallel to the direction of stretching, reducing the likelihood of observing scatterers. The stagnation of slabs within the transition zone is a common phenomenon in both simulation and observation. An increase in viscosity at the base of the mantle transition zone can effectively impede the sinking of the slab (Goes et al., 2017; Z.-H. Li et al., 2019), resulting in its stagnation. Additionally, the endothermic phase change from ringwoodite to post-spinel provides additional buoyancy, further delaying the slab descent through the transition zone by several tens of millions of years (Yanagisawa et al., 2010). Over time, variations in slab buoyancy, such as the arrival of continental lithosphere at the trench, can trigger the penetration of the slab into the lower mantle (Agrusta et al., 2017). Once slabs sink into the lower mantle, they gradually lose their original linear shape, potentially folding and/or buckling in the 1,500–2,000 km depth range (Domeier et al., 2016). We interpret our observations as indicative of a combination of these two processes, with the slab initially stagnating in the mantle transition zone before penetrating into the lower mantle and stagnating once again. Overall, our observation contributes further evidence to the stagnation, in addition to topographical irregularities.

The scatterers observed in the northeast are deeper than those in the southwest, suggesting the subduction of SEIS retreated southwestward beneath the southeast modern Indian Ocean, which used to be the Mesozoic Tethys Ocean. This trench retreat does not follow the well-understood tectonic history of the Indian Ocean following the breakup of East Gondwana (Pal & Ghosh, 2023). Beginning 130–140 Ma, Insular India separated from East Gondwana and traveled northeastward across the ancient Tethys Ocean to collide with Eurasia (Müller et al., 2022), opening the Indian Ocean. Thus, the subduction of SEIS is unlikely to have occurred during the long-term northeastern motion of India but likely ended before the early stages of the breakup of East Gondwana. The sinking of stagnant slabs in the mantle transition zone has been considered to last only about 50 Ma, even with a lower bound estimation for the subducted slab sinking rate through the entire mantle (1.3 ± 0.3 cm/yr) (Butterworth et al., 2014). Assuming the subduction of SEIS ended at 150 Ma, the stagnation of the slab in the mantle transition zone would have persisted for at least 100 Ma, which is longer than any other known slab on record (Agrusta et al., 2017). That prolonged stagnation observed aligns with some numerical simulations, specifically those considering the influences of the upward pull from a mid-ocean ridge or trench retreat (Gurnis et al., 1998;

19448007, 2024, 18, Downloaded from https://agupubs.onlinelibrary.wiley.com/doi/10.1029/2024GL110130 by University Of Southern California, Wiley Online Library on [12/11/2025]. See the Terms and Conditions (https://onlinelibrary.wiley.com/terms-and-conditions) on Wiley Online Library for rules of use; OA articles are governed by the applicable Creative Commons License

19448007, 2024, 18, Downloaded from https://agupubs.onlinelibrary.wiley.com/doi/10.1029/2024GL110130 by University Of Southern California, Wiley Online Library on [12/11/2025]. See the Terms and Conditions (https://onlinelibrary.wiley.com/terms-and-conditions) on Wiley Online Library for rules of use; OA articles are governed by the applicable Creative Commons License

Yanagisawa et al., 2010). However, determining the timing of the subduction for the 1,500 km deep stagnant slab remains challenging due to the potential contributions of both mantle convection (Ballmer et al., 2015; Tackley, 2012) and trench retreat to the horizontal displacement between the two parts of stagnation. It has been suggested that the upwelling mantle flow from African LLSVP could also influence the shape of the subducted slab (H. Wang et al., 2018). Consequently, whether the long-lasting trench retreat or the emergence of the mid-ocean ridge drives the long-term stagnation is still open to debate. Nonetheless, the coincident location of the present-day Southeast Indian Ridge (SEIR), which is right above the intersection between SEIS and the mantle transition zone (Figure 3b), could be interpreted that the upward pull from the mid-ocean ridge is most likely the principal mechanism driving the long-term stagnation of SEIS in the mantle transition zone. Despite uncertainty regarding the precise timing and mechanisms of the stagnation of SEIS, and whether other processes are involved in the generation of scatterers (e.g., delamination), our results provide additional constraints and insights for simulating and understanding the tectonic evolution of the Indian Ocean prior to 130–140 Ma and subduction in general.

Data Availability Statement

The LASA data used in this study is available on Zenodo (Zhang, 2024). The events used in this study are listed in Supplementary Table 1 in Supporting Information S1. Location of scattering points are provided in Supplementary Table 2 in Supporting Information S1.

Acknowledgments
We would like to thank Daniel A. Frost and the editor Daoyuan Sun for very careful reviews and insightful comments on this paper. P. Earle recovered the LASA data from deteriorating nine-track tapes in the 1990s, and S. Gibbons provided digital copies from his archives in 2019. Discussion with Xiyuan Bao and Mingqi Liu was helpful. This research was funded by NSF grant EAR-2041892 and by the Key Research Program of IGGCAS (Grant IGGCAS-201904 and IGGCAS-202204).

References

Agrusta, R., Goes, S., & van Hunen, J. (2017). Subducting-slab transition-zone interaction: Stagnation, penetration and mode switches. *Earth and Planetary Science Letters*, *464*, 10–23. https://doi.org/10.1016/j.epsl.2017.02.005

Agrusta, R., van Hunen, J., & Goes, S. (2018). Strong plates enhance mantle mixing in early earth. *Nature Communications*, *9*(1), 2708. https://doi.org/10.1038/s41467-018-05194-5

Ballmer, M. D., Schmerr, N. C., Nakagawa, T., & Ritsema, J. (2015). Compositional mantle layering revealed by slab stagnation at ˜1000-km depth. *Science Advances*, *1*(11), e1500815. https://doi.org/10.1126/sciadv.1500815

Becker, T. W., & Boschi, L. (2002). A comparison of tomographic and geodynamic mantle models. *Geochemistry, Geophysics, Geosystems*, *3*(1). https://doi.org/10.1029/2001GC000168

Butterworth, N. P., Talsma, A. S., Müller, R. D., Seton, M., Bunge, H. P., Schuberth, B. S. A., et al. (2014). Geological, tomographic, kinematic and geodynamic constraints on the dynamics of sinking slabs. *Journal of Geodynamics*, *73*, 1–13. https://doi.org/10.1016/j.jog.2013.10.006

Cao, A., & Romanowicz, B. (2007). Locating scatterers in the mantle using array analysis of PKP precursors from an earthquake doublet. *Earth and Planetary Science Letters*, *255*(1), 22–31. https://doi.org/10.1016/j.epsl.2006.12.002

Castle, J. C., & Creager, K. C. (1999). A steeply dipping discontinuity in the lower mantle beneath izu-bonin. *Journal of Geophysical Research*, *104*(B4), 7279–7292. https://doi.org/10.1029/1999JB900011

Domeier, M., Doubrovine, P. V., Torsvik, T. H., Spakman, W., & Bull, A. L. (2016). Global correlation of lower mantle structure and past subduction. *Geophysical Research Letters*, *43*(10), 4945–4953. https://doi.org/10.1002/2016GL068827

Dziewonski, A. M., & Anderson, D. L. (1981). Preliminary reference earth model. *Physics of the Earth and Planetary Interiors*, *25*(4), 297–356. https://doi.org/10.1016/0031-9201(81)90046-7

Earle, P. S. (2002). Origins of high-frequency scattered waves near pkkp from large aperture seismic array data. *Bulletin of the Seismological Society of America*, *92*(2), 751–760. https://doi.org/10.1785/0120010169

Frosch, R., & Green, P. (1966). The concept of a large aperture seismic array. *Proceedings of the Royal Society of London - Series A: Mathematical and Physical Sciences*, *290*(1422), 368–384. https://doi.org/10.1098/rspa.1966.0056

Frost, D. A., Rost, S., Selby, N. D., & Stuart, G. W. (2013). Detection of a tall ridge at the core–mantle boundary from scattered PKP energy. *Geophysical Journal International*, *195*(1), 558–574. https://doi.org/10.1093/gji/ggt242

Gerya, T. V., Bercovici, D., & Becker, T. W. (2021). Dynamic slab segmentation due to brittle–ductile damage in the outer rise. *Nature*, *599*(7884), 245–250. https://doi.org/10.1038/s41586-021-03937-x

Gibbons, A. D., Whittaker, J. M., & Müller, R. D. (2013). The breakup of East Gondwana: Assimilating constraints from Cretaceous ocean basins around India into a best-fit tectonic model. *Journal of Geophysical Research: Solid Earth*, *118*(3), 808–822. https://doi.org/10.1002/jgrb.50079

Goes, S., Agrusta, R., van Hunen, J., & Garel, F. (2017). Subduction-transition zone interaction: A review. *Geosphere*, *13*(3), 644–664. https://doi.org/10.1130/GES01476.1

Grand, S. P. (2002). Mantle shear–wave tomography and the fate of subducted slabs. *Philosophical Transactions of the Royal Society of London, Series A: Mathematical, Physical and Engineering Sciences*, *360*(1800), 2475–2491. https://doi.org/10.1098/rsta.2002.1077

Gurnis, M., Müller, R. D., & Moresi, L. (1998). Cretaceous vertical motion of Australia and the AustralianAntarctic discordance. *Science*, *279*(5356), 1499–1504. https://doi.org/10.1126/science.279.5356.1499

Isacks, B., & Molnar, P. (1971). Distribution of stresses in the descending lithosphere from a global survey of focal-mechanism solutions of mantle earthquakes. *Reviews of Geophysics*, *9*(1), 103–174. https://doi.org/10.1029/RG009i001p00103

Ishii, T., Miyajima, N., Criniti, G., Hu, Q., Glazyrin, K., & Katsura, T. (2022). High pressure-temperature phase relations of basaltic crust up to mid-mantle conditions. *Earth and Planetary Science Letters*, *584*, 117472. https://doi.org/10.1016/j.epsl.2022.117472

Kaneshima, S. (2003). Small-scale heterogeneity at the top of the lower mantle around the mariana slab. *Earth and Planetary Science Letters*, *209*(1–2), 85–101. https://doi.org/10.1016/S0012-821X(03)00048-7

Kaneshima, S. (2013). Lower mantle seismic scatterers below the subducting Tonga slab: Evidence for slab entrainment of transition zone materials. *Physics of the Earth and Planetary Interiors*, *222*, 35–46. https://doi.org/10.1016/j.pepi.2013.07.001

Kaneshima, S. (2016). Seismic scatterers in the mid-lower mantle. *Physics of the Earth and Planetary Interiors*, *257*, 105–114. https://doi.org/10.1016/j.pepi.2016.05.004

Kennet, B. (1991). Iaspei 1991 seismological tables. *Terra Nova*, *3*(2), 122. https://doi.org/10.1111/j.1365-3121.1991.tb00863.x
Korenaga, J. (2015). Constraining the geometries of small-scale heterogeneities: A case study from the mariana region. *Journal of Geophysical Research: Solid Earth*, *120*(11), 7830–7851. https://doi.org/10.1002/2015JB012432
Lay, T. (1994). The fate of descending slabs. *Annual Review of Earth and Planetary Sciences*, *22*(1), 33–61. https://doi.org/10.1146/annurev.ea.22.050194.000341
Li, J., & Yuen, D. A. (2014). Mid-mantle heterogeneities associated with izanagi plate: Implications for regional mantle viscosity. *Earth and Planetary Science Letters*, *385*, 137–144. https://doi.org/10.1016/j.epsl.2013.10.042
Li, Z.-H., Gerya, T., & Connolly, J. A. (2019). Variability of subducting slab morphologies in the mantle transition zone: Insight from petrological-thermomechanical modeling. *Earth-Science Reviews*, *196*, 102874. https://doi.org/10.1016/j.earscirev.2019.05.018
Mao, W., Gurnis, M., & Wu, W. (2022). On the origin of small-scale seismic scatters at 660-km depth. *Geochemistry, Geophysics, Geosystems*, *23*(12), e2022GC010560. https://doi.org/10.1029/2022GC010560
Müller, R. D., Flament, N., Cannon, J., Tetley, M. G., Williams, S. E., Cao, X., et al. (2022). A tectonic-rules-based mantle reference frame since 1 billion years ago – Implications for supercontinent cycles and plate–mantle system evolution. *Solid Earth*, *13*(7), 1127–1159. https://doi.org/10.5194/se-13-1127-2022
Niu, F. (2014). Distinct compositional thin layers at mid-mantle depths beneath northeast China revealed by the USArray. *Earth and Planetary Science Letters*, *402*, 305–312. https://doi.org/10.1016/j.epsl.2013.02.015
Niu, F., Kawakatsu, H., & Fukao, Y. (2003). Seismic evidence for a chemical heterogeneity in the midmantle: A strong and slightly dipping seismic reflector beneath the mariana subduction zone. *Journal of Geophysical Research*, *108*(B9). https://doi.org/10.1029/2002JB002384
Pal, D., & Ghosh, A. (2023). How the Indian ocean geoid low was formed. *Geophysical Research Letters*, *50*(9), e2022GL102694. https://doi.org/10.1029/2022GL102694
Ringwood, A. E., & Irifune, T. (1988). Nature of the 650–km seismic discontinuity: Implications for mantle dynamics and differentiation. *Nature*, *331*(6152), 131–136. https://doi.org/10.1038/331131a0
Rochira, F., Schumacher, L., & Thomas, C. (2022). Mapping the edge of subducted slabs in the lower mantle beneath southern Asia. *Geophysical Journal International*, *230*(2), 1239–1252. https://doi.org/10.1093/gji/ggac110
Romanowicz, B., & Mitchell, B. (2015). 1.25-deep earth structure: Q of the earth from crust to core. *Treatise on geophysics*, *1*, 789–827. https://doi.org/10.1016/B978-0-444-53802-4.00021-X
Rost, S., Earle, P. S., Shearer, P. M., Frost, D. A., & Selby, N. D. (2015). Seismic detections of small-scale heterogeneities in the deep earth. In *The Earth's heterogeneous mantle: A geophysical, geodynamical, and geochemical perspective* (pp. 367–390). Springer International Publishing. https://doi.org/10.1007/978-3-319-15627-9_12
Rost, S., & Thomas, C. (2002). Array seismology: Methods and applications. *Reviews of Geophysics*, *40*(3), 2–27. https://doi.org/10.1029/2000RG000100
Shi, Y., Wei, D., Li, Z.-H., Liu, M.-Q., & Liu, M. (2019). Subduction mode selection during slab and mantle transition zone interaction: Numerical modeling. *Earthquakes and Multi-hazards Around the Pacific Rim*, *II*, 5–24. https://doi.org/10.1007/978-3-319-92297-3_2
Simmons, N. A., Myers, S. C., Johannesson, G., & Matzel, E. (2012). LLNL-G3Dv3: Global P wave tomography model for improved regional and teleseismic travel time prediction. *Journal of Geophysical Research*, *117*(B10). https://doi.org/10.1029/2012JB009525
Simmons, N. A., Myers, S. C., Johannesson, G., Matzel, E., & Grand, S. P. (2015). Evidence for long-lived subduction of an ancient tectonic plate beneath the southern Indian Ocean. *Geophysical Research Letters*, *42*(21), 9270–9278. https://doi.org/10.1002/2015GL066237
Tackley, P. J. (2002). Strong heterogeneity caused by deep mantle layering. *Geochemistry, Geophysics, Geosystems*, *3*(4), 1–22. https://doi.org/10.1029/2001GC000167
Tackley, P. J. (2012). Dynamics and evolution of the deep mantle resulting from thermal, chemical, phase and melting effects. *Earth-Science Reviews*, *110*(1–4), 1–25. https://doi.org/10.1016/j.earscirev.2011.10.001
Vidale, J. E. (2019). Very slow rotation of Earth's inner core from 1971 to 1974. *Geophysical Research Letters*, *46*(16), 9483–9488. https://doi.org/10.1029/2019GL083774
Wang, H., Wang, Y., Gurnis, M., Zahirovic, S., & Leng, W. (2018). A long-lived indian ocean slab: Deep dip reversal induced by the african llsvp. *Earth and Planetary Science Letters*, *497*, 1–11. https://doi.org/10.1016/j.epsl.2018.05.050
Wang, W., & Vidale, J. E. (2022a). An initial map of fine-scale heterogeneity in the Earth's inner core. *Nature Geoscience*, *15*(3), 240–244. https://doi.org/10.1038/s41561-022-00903-8
Wang, W., & Vidale, J. E. (2022b). Seismological observation of Earth's oscillating inner core. *Science Advances*, *8*(23), eabm9916. https://doi.org/10.1126/sciadv.abm9916
Wei, S. S., Shearer, P. M., Lithgow-Bertelloni, C., Stixrude, L., & Tian, D. (2020). Oceanic plateau of the Hawaiian mantle plume head subducted to the uppermost lower mantle. *Science*, *370*(6519), 983–987. https://doi.org/10.1126/science.abd0312
Wen, L. (2000). Intense seismic scattering near the Earth's core-mantle boundary beneath the Comoros hotspot. *Geophysical Research Letters*, *27*(22), 3627–3630. https://doi.org/10.1029/2000GL011831
Xu, W., Lithgow-Bertelloni, C., Stixrude, L., & Ritsema, J. (2008). The effect of bulk composition and temperature on mantle seismic structure. *Earth and Planetary Science Letters*, *275*(1–2), 70–79. https://doi.org/10.1016/j.epsl.2008.08.012
Yanagisawa, T., Yamagishi, Y., Hamano, Y., & Stegman, D. R. (2010). Mechanism for generating stagnant slabs in 3-D spherical mantle convection models at Earth-like conditions. *Physics of the Earth and Planetary Interiors*, *183*(1), 341–352. https://doi.org/10.1016/j.pepi.2010.02.005
Yang, Z., & He, X. (2015). Oceanic crust in the mid-mantle beneath west-central pacific subduction zones: Evidence from s to p converted waveforms. *Geophysical Journal International*, *203*(1), 541–547. https://doi.org/10.1093/gji/ggv314
Zhang, H. (2024). *LASA* data - P*PKP. [dataset]. *Zenodo*. https://doi.org/10.5281/zenodo.11145160
Zhao, D., Yamamoto, Y., & Yanada, T. (2013). Global mantle heterogeneity and its influence on teleseismic regional tomography. *Gondwana Research*, *23*(2), 595–616. https://doi.org/10.1016/j.gr.2012.08.004

19448007, 2024, 18, Downloaded from https://agupubs.onlinelibrary.wiley.com/doi/10.1029/2024GL110130 by University Of Southern California, Wiley Online Library on [12/11/2025]. See the Terms and Conditions (https://onlinelibrary.wiley.com/terms-and-conditions) on Wiley Online Library for rules of use; OA articles are governed by the applicable Creative Commons License